Available online at www.sciencedirect.com
ScienceDirect
Ceramics International 37 (2011) 1819–1824
CERAMICS INTERNATIONAL
www.elsevier.com/locate/ceramint

Fabrication and characterization of bioactive glass/hydroxyapatite nanocomposite foam by gelcasting method

H. Ghomi *, M.H. Fathi, H. Edris

Biomaterials Group, Department of Materials Engineering, Isfahan University of Technology, Isfahan 8415683111, Iran

Received 4 October 2010; received in revised form 25 October 2010; accepted 30 January 2011
Available online 9 March 2011

Abstract

Bioceramic foams have been applied for drug releasing agents, cell loading, and widely for hard tissue scaffold. The aim of this study was fabrication and characterization of nanostructure bioceramic composite foam (BCF) consisting of hydroxyapatite (HA) and bioactive glass (BG) via gelcasting method for applications in tissue engineering. X-ray diffraction (XRD), scanning electron microscopy (SEM), and transmission electron microscopy (TEM) analysis techniques were utilized in order to evaluate respectively, phase composition, dimension, morphology, and interconnectivity of pores, and particle size of synthesized HA, BG, and BCF. The results showed that fabrication of the BCF with a particle size in the range 20–42 nm and pore size in the range 100–250 μm was successfully performed. The maximum values of compressive strength and elastic modulus of the BCF were found to be about 1.95 MPa and 204 MPa, respectively, related to a sample sintered at 900 °C for 4 h. The mean values of the true (total) and apparent (interconnected) porosity were calculated in the range 86–91% and 60–71%, respectively. It seems that the measured properties make the BCF a good candidate for tissue engineering applications, preferentially in drug delivery, cell loading, and other nonloading applications.

Keywords: A. Sol–gel processes; B. Nanocomposites; B. Porosity; E. Biomedical applications

1. Introduction

The main purpose in tissue engineering is the stimulation of the body's own mechanisms to reconstruct diseased or damaged tissue to its original state and function. Bone and cartilage are tissues that due to trauma, tumors removal, or more commonly, age-related diseases such as osteoporosis and osteoarthritis are often in need of regeneration [1]. On the other hand the use of traditional methods such as autografts, allografts, and xenografts for this purpose have the important limitations of low availability, no mechanical strength and shape, second site morbidity, and disease transmission like hepatitis and HIV. Thus, with such critical arguments on applications of naturally derived bone grafts, development of artificial bone substitution materials made from metals, ceramics, polymers, and composites are of a great importance [1–3].

Porous bioceramics have found various applications in tissue engineering. Therefore, different methods have been developed for fabrication of these porous bioceramics, including polymeric sponge method, conversion of natural bones, ceramic foaming technique, gelcasting of foams, starch consolidation, microwave processing, slip casting, and electrophoretic deposition technique [4]. Among these methods, the gelcasting method has important advantages such as complex shaping capability, good dimensional accuracy, uniform structure, and high strength [5]. In this method, slurry is made of ceramic powder, dispersant, surfactant, and gelling agent and foaming is conducted through vigorous agitation [5,6]. The foamed slurry is poured into the mold, the gelation is performed by cooling the foam (for biopolymeric and organic gelling agent) [5,6] or heating the foam (for monomer solution) [7]. The foam is then de-molded, dried, and finally sintered.

Many researchers have fabricated bioceramic foams, but their produced foams had micro-sized structure [5–7]. Nanostructure materials in comparison to the same composition of microstructure materials have better magnetical, optical, electrical, and mechanical properties. These materials contain large fraction of defects like grain boundaries, inter phase boundary, and dislocations. This has a great effect on physical and mechanical properties of the final product. In addition,

* Corresponding author. Tel.: +98 311 3912750; fax: +98 311 3912752.
E-mail address: hamed1985.gh@gmail.com (H. Ghomi).

0272-8842/$36.00
doi:10.1016/j.ceramint.2011.03.002

nanostructure ceramics are stronger and tougher than large grain ceramics. Nanostructure hydroxyapatite (HA) and bioactive glass (BG), due to their higher surface to volume ratio and similarity with nano-sized HA existing in the bone, could control protein interactions (for example, adsorption, configuration, and bioactivity); therefore, modulating subsequent enhanced osteoblast adhesion [8].

Considering benefits of nanostructure bioceramics, this study focused on fabrication of nanostructure bioceramic composite foam (BCF). For this purpose, HA and BG nanopowders were synthesized by the sol–gel method and porous body of HA/BG composite was fabricated by the gelcasting technique.

2. Experimental procedure

2.1. Starting materials

The chemical materials used in this study were tetraethyl orthosilicate (TEOS, Merck), triethyl phosphate (TEP, Aldrich), calcium nitrate tetrahydrate ($Ca(NO_3)_2{\cdot}4H_2O$, Merck), phosphoric pentoxide (P_2O_5, Merck), absolute ethanol (C_2H_5OH, Merck), hydrochloric acid (HCl, Merck), agarose powder (Merck), Tergitol (Aldrich), tripoly phosphate sodium (TPP), and deionized water.

2.2. Preparation of HA nanopowder

In order to prepare nanopowder HA by the sol–gel method, absolute ethanol was used as the solvent. The desired amounts of calcium nitrate tetrahydrate and phosphoric pentoxide were dissolved separately in ethanol to form 1.67 and 0.5 mol/l solutions, respectively. The prepared solutions were mixed together in a Ca/P molar ratio of 1.67 as an initial mixed precursor solution. Then the mixture was stirred at ambient temperature for about 24 h to obtain a white transparent gel. As-formed gel was then aged at room temperature for 24 h and dried at 80 °C in an electrical air oven for 24 h. The dried gel was sintered at 600 °C for 2 min in a muffle furnace by a heating rate of 5 °C/min, and was placed in air for cooling to ambient temperature.

2.3. Preparation of BG nanopowder

For preparing nanopowder BG, the sol–gel preparation was carried out using the BG composition that belongs to the system $CaO–SiO_2–P_2O_5$: 63S with 65 mol% SiO_2, 31 mol% CaO, and 4 mol% P_2O_5. For this purpose sufficient amounts of TEOS, deionized water, and 2 N HCl were dissolved in ethanol by stirring at room temperature for 30 min. TEP was then dissolved into the prepared sol. After stirring for 20 min, the $Ca(NO_3)_2{\cdot}4H_2O$ was added into the sol and stirred for one more hour. The obtained sol was then aged at 60 °C for 48 h and dried at 120 °C in an electrical air oven for 48 h. The dried gel was sintered at 600 °C for 2 h in a muffle furnace by a heating rate of 10 °C/min. Then it was placed in air for cooling to ambient temperature.

2.4. Preparation of HA/BG composite foams

A solution of 1 wt.% tripoly phosphate sodium in deionized water was prepared as a dispersant. The uses of dispersants are necessary to form highly fluid slurry with maximum solid loading that lead to increasing the strength of the foam. Then a mixture of 50 wt.% HA and 50 wt.% BG nanopowder was prepared by ball milling (B/P: 5/1, rotational speed: 175 rpm, and time: 45 min). This powder mixture was added to the solution to reach a solid loading of 60 wt.% and was stirred for 15 min by a magnetic stirrer. Moreover, a solution of agarose (7 wt.%) was prepared by mixing agarose powder with deionized water followed by heating up to 130 °C. The agarose solution was added to HA/BG slurry to obtain a suspension with 50 wt.% HA/BG and 1.2 wt.% active gelling agent (agarose). During the addition of the agarose solution to HA/BG slurry, the temperature of all constituents was maintained at 80 °C. Then 3 vol.% Tergitol was added to the suspension as a surfactant. The surfactant stabilizes the foams before the permanent stabilizing by the gelation of gelling agent. Foaming was conducted through agitation by the help of a triple-blade mixer at 80 °C. The foamed slurry was poured into the polyethylene mold and gelation was performed by cooling the foam to 0 °C. The samples were then de-molded, dried in room temperature, and sintered at different temperatures for 4 h.

2.5. Materials characterization

2.5.1. X-ray diffraction analyses

Phase structure analyses were carried out by X-ray diffractometer (XRD, Philips Xpert) using Ni filtered Cu kα (λ Cu kα = 0.154186 nm, radiation at 30 mA, and 40 kV) over the 2θ range of 20–70° (step size: 0.05 and time per step: 1 s). The obtained experimental patterns were compared to the standards, compiled by joint committee on powder diffraction and standards (JCDPS).

The crystallite size of the prepared powders and composite foams was estimated by broadening of XRD peaks using Scherrer's formula [9]:

$$d = \frac{0.89\lambda}{B\cos\theta} \quad (1)$$

where d is the crystallite size (nm), λ is the wavelength of the X-ray (nm), B is the full width of diffraction peak under consideration (rad) in the middle of its height, and θ is Bragg's angle (°).

2.5.2. Electron microscopy analyses

The morphology and agglomerates size distribution of the powders, morphology and size of the pores, and composition of the composite foams were investigated by scanning electron microscopy (SEM, Phillips XL 30: Eindhoven, The Netherlands) equipped with EDS analyser utilizing ZAF corrections.

The particle sizes of the prepared foams were analysed by transmission electron microscopy (TEM, Phillips CM-200).

2.5.3. Porosity measurement and mechanical testing

The porosity of the bulk specimens was measured by Archimedes method. The apparent or interconnected porosity is determined by weighing the dry ceramic (W_d), then reweighing the ceramic both when it is suspended in water (W_s) and after it is removed from the water (W_w). Then

$$\text{Apparent porosity} = \left[\frac{W_w - W_d}{W_w - W_s}\right] \times 100 \quad (2)$$

The true porosity includes both interconnected and closed pores. The true porosity is

$$\text{True porosity} = \left[\frac{\rho - B}{\rho}\right] \times 100 \quad (3)$$

where B is the bulk density and ρ is the true density or specific gravity of the ceramic. The bulk density is the weight of the ceramic divided by its volume [10].

$$B = \frac{W_d}{W_w - W_s} \quad (4)$$

In order to determine the mechanical properties of bioceramic foams, a good criterion is applying the compression test. For this purpose, the compressive tests were performed on samples consisting of cylindrical bars (10 mm in diameter and 20 mm in length) which were loaded at a crosshead speed of 0.5 mm/min using a universal testing machine (zwick, material prufung, 1446-60). The load was maintained until the first crack appeared on the foam. Results were based on an average of five samples.

3. Results and discussion

Fig. 1(a and b) shows the XRD patterns of the initial BG and HA nanopowders. The other three XRD paterns shown in Fig. 1(c–e) are related to the composite foams sintered at 700, 800, and 900 °C for 4 h. By increasing the sintering temperature to 900 °C, the calcium phosphate peaks appeared in the composite foam XRD pattern. Since calcium phosphate is a bioactive and biodegradable phase, it is not undesirable and even in drug delivery and bone tissue engineering, is a beneficial phase. The crystallite size of the composite foams was estimated by broadening of XRD peaks using Scherrer's formula in the range 24–38 nm.

SEM micrographs of the prepared foam in Fig. 2 show the morphology, size, and interconnectivity of pores. As can be seen from Fig. 2, the size of the pores was between 100 and 250 μm, appropriate for biomedical applications. In addition, Fig. 2 clearly shows interconnectivity between the pores. Potoczek et al. produced HA and calcium phosphate foams with pore size in the range 130–380 μm and 350–900 μm, respectively [5,6]. Ramay and coworkers obtained HA foams with the pore size in the range 200–400 μm [11]. Since, minimum pore size required to enable ingrowth of surrounding bone with blood supply, is about 100–150 μm [12,13] and with larger pores the strength of the foams decreases significantly [4], obtaining the minimum pore size capable of filling with surrounding bones is very important.

To determine the true and apparent porosity of the composite foams, three samples of the foams were selected for each sintering temperature and the mean values of true and apparent porosity were calculated in the range 86–91% and 60–71%, respectively. The maximum values in the ranges are related to minimum sintering temperature.

The mean values of compressive strength and elastic modulus of the composite foams were measured in the range 0.87–1.95 MPa and 92–204 MPa. The maximum values are for the sample sintered at 900 °C for 4 h. Therefore, it is obvious that less porosity and pore size increases the two mechanical properties mentioned above. Potoczek and coworker's compressive strength results for HA foams porosity in the range 73–92% were 0.8–5.9 MPa [5]. Their results for the calcium phosphate foams porosity up to 90% were 0.44–1.92 MPa [6]. Sepulveda et al. fabricated the HA foams with porosity and compressive strength in the range 72–90% and 1.6–5.8 MPa [7]. According to this result, the foams compressive strength has increased with decreasing the particle size and production of BG reinforced HA. Furthermore, decreasing particle size through increasing the specific surface area facing the body fluid causes to enhance the osteoblast functions, which are proliferation, alkaline phosphatase synthesis, and calcium containing mineral deposition [14–16].

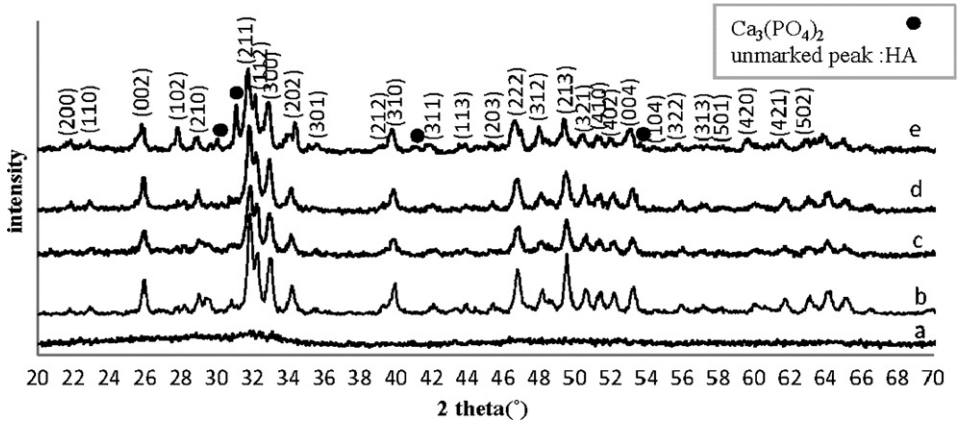

Fig. 1. XRD patterns of the prepared (a) BG nanopowder, (b) HA nanopowder, (c–e) composite foams at different sintering temperature, 700 °C, 800 °C, and 900 °C for 4 h, respectively.

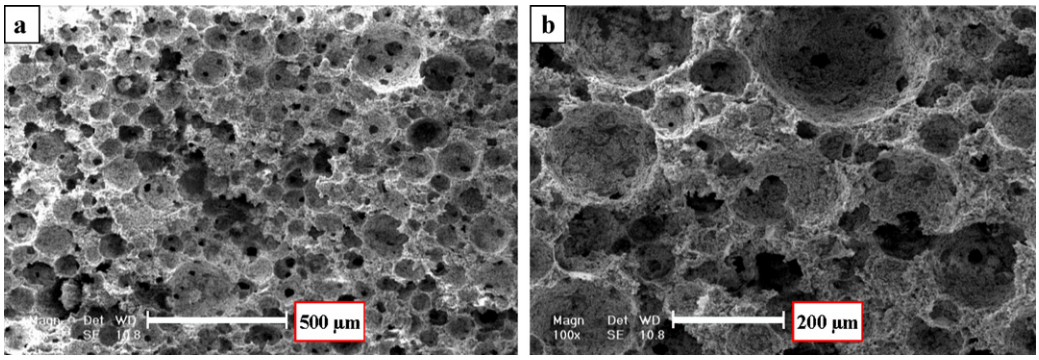

Fig. 2. SEM micrographs of the composite foam sintered at 900 °C for 4 h at different magnifications.

As shown in Fig. 3, the existence of calcium, phosphorus, carbon, oxygen, and silicon in EDS analysis are related to carbonate hydroxyapatite and bioactive glass.

Fig. 4 shows TEM micrographs of the sintered foam at 900 °C, illustrating the particle size to be about 20–42 nm. This is in agreement with obtained results of XRD patterns (24–38 nm).

Bioceramics as a class of biomaterials are important for biomedical applications [17]. Porous bioceramic implants or devices have been paid much attention. In fact, porous bioceramics have been used for bone defect filling, implant fixation via bone ingrowth (i.e. biological fixation), bone regeneration via tissue engineering [4,18,19], drug delivery [20–23], cell loading [24,25], and ocular implant [26]. Porous bioceramics such as HA and BG are the best candidates for using in bone tissue engineering due to their similar chemical composition to the mineral phase of bone specially that of HA, excellent biocompatibility to bone tissue, and good bioactivity especially that of BG that able to bond with hard and soft tissue [4,17,27,28]. Furthermore, porous bioceramics have a high surface area that leads to excellent osteoconductivity and biodegradability providing fast bone ingrowth [4]. Their high surface area increases cell adhesion to the scaffold and so promotes bone tissue reconstruction. In addition, the growth of

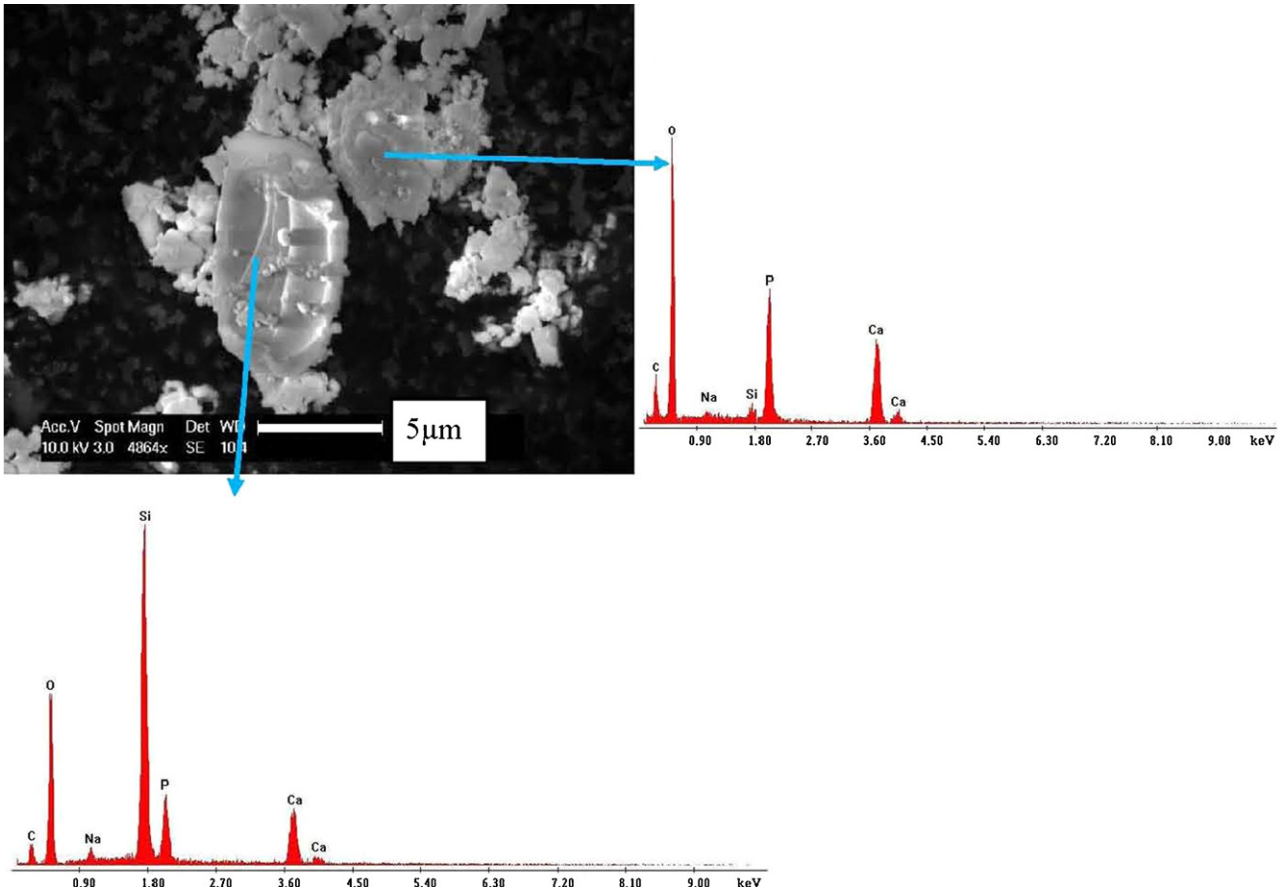

Fig. 3. EDS spectrum of the composite foam sintered at 900 °C for 4 h.

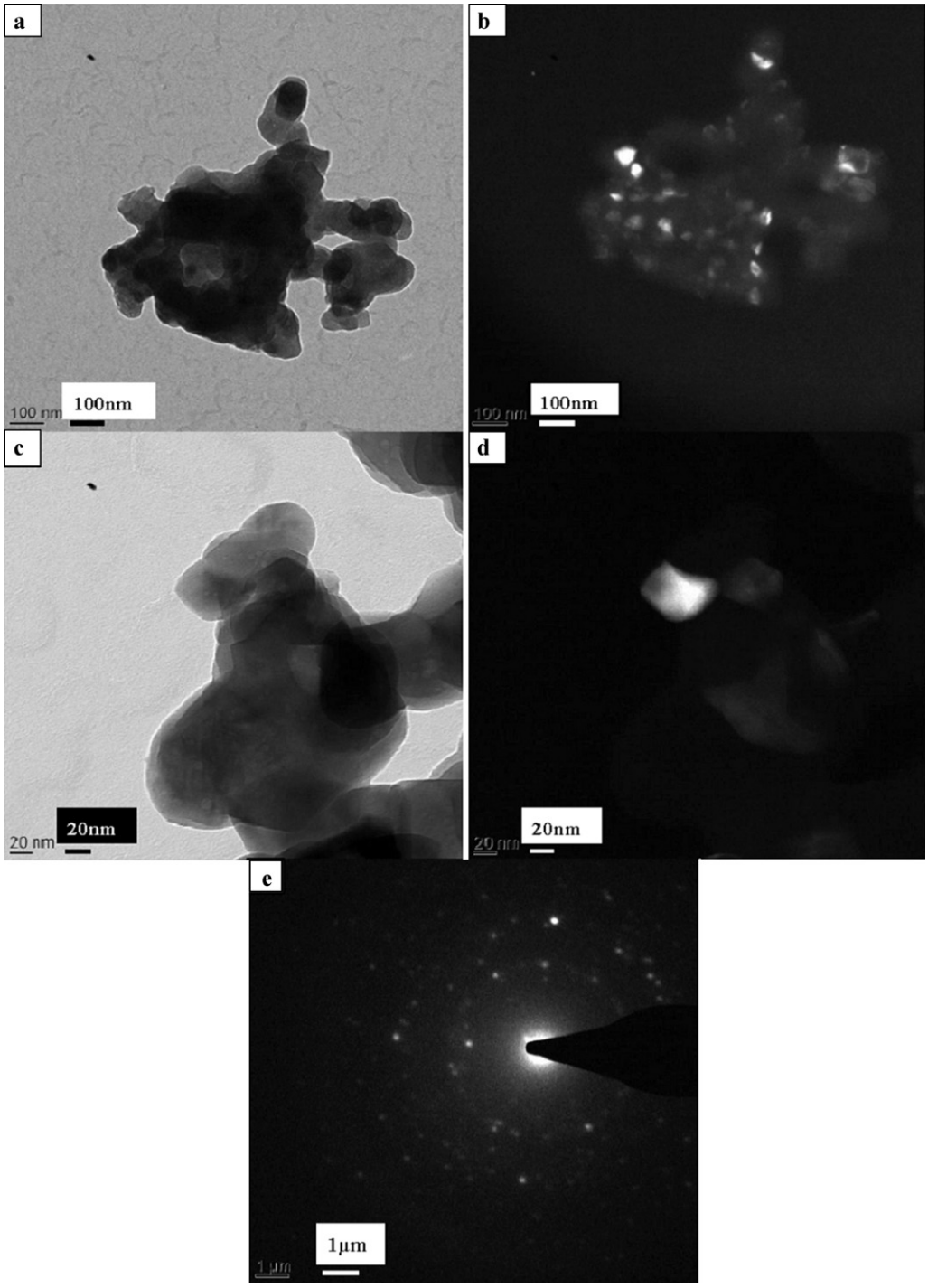

Fig. 4. TEM micrographs of the composite foam sintered at 900 °C for 4 h at different magnifications.

bone tissue into the pores leads to increasing strength of the implant [4,28]. Yoshikawa and coworkers denoted that the compressive strength of porous HA increases from 2 to 20 MPa after 3 months implantation [29]. It was realized that appropriate scaffold for application in tissue engineering should have appropriate pore size, pore interconnectivity, biocompatibility, osteoconductivity, mechanical strength, and biodegradability. Interconnectivity of the pore is necessary for allowing circulation and exchange of body fluids, ion diffusion, nutritional supply, osteoblast cell penetration, and vascularization [4,30].

The manufactured BCF, because of its sufficient pore size, compressive strength, and interconnectivity between pores, could be a good candidate to use in tissue engineering. Its high porosity level and nano-sized structure increase the specific surface and so the bioreactions will significantly increase. On the other hand, by changing the ratio of HA/BG, it can reach the appropriate bioactivity and biodegradability level needed for different applications.

Further studies will be focused on cell culture and in vivo tests on the prepared foams, composite foams fabrication with

different composition and comparison of their properties with the single phase foams of HA and BG.

4. Conclusion

In this research BCF with a particle and pore size in the range 20–42 nm and 100–250 μm, respectively, was fabricated. The mean values of compressive strength and elastic modulus of the composite foams were measured in the range 0.87–1.95 MPa and 92–204 MPa. The maximum values in the ranges belong to the sample sintered at 900 °C for 4 h. The mean values of true and apparent porosity were calculated in the range 86–91% and 60–71%, respectively. The maximum values in the ranges are related to minimum sintering temperature. It seems that, manufactured foam could be a good candidate for tissue engineering applications, preferentially in drug delivery, cell loading, and other nonloading applications, but cell culture and in vivo tests are needed for more assurance.

Acknowledgements

The authors are grateful for support of this research by Isfahan University of Technology.

References

[1] J.R. Jones, E. Gentleman, J. Polak, Bioactive glass scaffolds for bone regeneration, J. Elements 3 (2007) 393–399.
[2] B.D. Ratner, A.S. Hoffman, Biomaterials Science: An Introduction to Materials in Medicine, Elsevier Science & Technology, 2004.
[3] R. Lanza, R. Langer, J.P. Vacanti, Principles of Tissue Engineering, R.G. Landes Company and Academic Press Inc., Texas, Austin, 1997.
[4] I. Sopyan, M. Mel, S. Ramesh, K.A. Khalid, Porous hydroxyapatite for artificial bone applications, Sci. Technol. Adv. Mater. 8 (2007) 116–123.
[5] M. Potoczek, Hydroxyapatite foams produced by gelcasting using agarose, Mater. Lett. 62 (2008) 1055–1057.
[6] M. Potoczek, A. Zima, Z. Paszkiewicz, A. Slosarczyk, Manufacturing of highly porous calcium phosphate bioceramics via gel-casting using agarose, Ceram. Int. 35 (2009) 2249–2254.
[7] P. Sepulveda, F.S. Ortega, M.D.M. Innocentini, V.C. Pandolfelli, Properties of highly porous hydroxyapatite obtained by the gelcasting of foams, J. Am. Ceram. Soc. 83 (2000) 3021–3024.
[8] M.P. Ferraz, F.J. Monteiro, C.M. Manuel, Hydroxyapatite nanoparticles: a review of preparation methodologies, J. Appl. Biomater. Biomech. 2 (2004) 74–80.
[9] B.D. Cullity, Elements of X-Ray Diffraction, 2nd ed., Addison-Wesley, 1978.
[10] R.D. Askeland, The Science and Engineering of Materials, 2nd ed., PWS Pub. Co., 1989.
[11] H.R. Ramay, M. Zhang, Preparation of porous hydroxyapatite scaffolds by combination of the gel-casting and polymer sponge methods, Biomaterials 24 (2003) 3293–3302.
[12] S.F. Hulbert, S.J. Morisson, J.J. Klawitter, Tissue reaction to three ceramics of porous and non-porous structures, J. Biomed. Mater. Res. 6 (1972) 347–374.
[13] S.F. Hulbert, J.J. Klawitter, R.B. Leonard, in: W.W. Kriegel, H. Palmour (Eds.), Compatibility of Bioceramics with Physiological Environment Ceramics in Serve Environments, Plenum Press, New York, 1971, pp. 417–434.
[14] T.J. Webster, R.W. Siegel, R. Bizios, Enhanced surface and mechanical properties of nanophase ceramics to achieve orthopaedic/dental implant efficacy, Key Eng. Mater. 192–195 (2001) 321–324.
[15] T.J. Webster, R.W. Siegel, R. Bizios, Enhanced functions of osteoblasts on nanophase ceramics, Biomaterials 21 (2000) 1803–1810.
[16] T.J. Webster, C. Ergun, R.H. Doremus, R.W. Siegel, R. Bizios, Specific proteins mediate enhanced osteoblast adhesion on nanophase ceramics, J. Biomed. Mater. Res. 5 (2000) 475–483.
[17] S. Oh, N. Oh, M. Appleford, J.L. Ong, Bioceramics for tissue engineering applications, Am. J. Biochem. Biotechnol. 2 (2006) 49–56.
[18] Z.C. Qizhi, D.T. Ian, R.B. Aldo, 45S5 bioglass derived glass–ceramic scaffolds for bone tissue engineering, Biomaterials 27 (2006) 2414–2425.
[19] L.L. Hench, Bioactive glass and hybrid scaffolds prepared by sol–gel method for bone tissue engineering, J. Am. Ceram. Soc. 81 (1998) 1705–1728.
[20] A. Krajewski, A. Ravaglioli, E. Roncari, P. Pinasco, Porous ceramic bodies for drug delivery, J. Mater. Sci. Mater. Med. 12 (2000) 763–771.
[21] D.J.A. Netz, P. Sepulveda, V.C. Pandolfelli, A.C.C. Spadaro, J.B. Alencastre, M.V.L.B. Bentley, et al., Potential use of gelcasting hydroxyapatite porous ceramic as an implantable drug delivery system, Int. J. Pharm. 213 (2001) 117–125.
[22] S. Hesaraki, F. Moztarzadeh, N. Nezafati, Evaluation of a bioceramic-based nanocomposite material for controlled delivery of a non-steroidal anti-inflammatory drug, Med. Eng. Phys. 31 (2009) 1205–1213.
[23] M. Itokazu, M. Esaki, K. Yamamoto, T. Tanemori, T. Kasai, Local drug delivery system using ceramics: vacuum method for impregnating a chemotherapeutic agent into a porous hydroxyapatite block, J. Mater. Sci. Mater. Med. 10 (1999) 249–252.
[24] H. Ohgushi, A.I. Caplan, Stem cell technology and bioceramics: from cell to gene engineering, J. Biomed. Mater. 48 (1999) 913–927.
[25] A. Banfi, A. Muraglia, B. Dozin, M. Mastrogiacomo, R. Cancedda, R. Quarto, Proliferation kinetics and differentiation potential of ex vivo expanded human bone marrow stromal cells: implications for their use in cell therapy, Exp. Hematol. 28 (2000) 707–715.
[26] B. Kundu, M.K. Sinha, M.K. Mitra, D. Basu, Fabrication and characterization of porous hydroxyapatite ocular implant followed by an in vivo study in dogs, Bull. Mater. Sci. 27 (2004) 133–140.
[27] M.H. Fathi, A. Doost Mohammadi, Preparation and characterization of sol–gel bioactive glass coating for improvement of biocompatibility of human body implant, Mater. Sci. Eng. 474 (2008) 128–133.
[28] M.H. Fathi, A. Hanifi, Evaluation and characterization of nanostructure hydroxyapatite powder prepared by simple sol–gel method, Mater. Lett. 67 (2007) 3978–3983.
[29] H. Yoshikawa, A. Myiui, Bone tissue engineering with porous hydroxyapatite ceramics, J. Artif. Organs 8 (2005) 131–136.
[30] J.R. Jones, L.L. Hench, Effect of surfactant concentration and composition on the structure and properties of sol–gel-derived bioactive glass foam scaffolds for tissue engineering, J. Mater. Sci. 38 (2003) 3783–3790.